Lipid and carotenoid cooperation-driven adaptation to light and temperature stress in *Synechocystis* sp. PCC6803

Tomas Zakar [a,1], Eva Herman [a,1], Sindhujaa Vajravel [a], Laszlo Kovacs [a], Jana Knoppová [b], Josef Komenda [b], Ildiko Domonkos [a], Mihaly Kis [a], Zoltan Gombos [a], Hajnalka Laczko-Dobos [a,*]

[a] *Institute of Plant Biology, Biological Research Centre, Hungarian Academy of Sciences, H-6701 Szeged, Hungary*
[b] *Centre Algatech, Institute of Microbiology, Academy of Sciences, 37981 Treboň, Czech Republic*

ARTICLE INFO

ABSTRACT

Polyunsaturated lipids are important components of photosynthetic membranes. Xanthophylls are the main photoprotective agents, can assist in protection against light stress, and are crucial in the recovery from photoinhibition. We generated the xanthophyll- and polyunsaturated lipid-deficient ROAD mutant of *Synechocystis* sp. PCC6803 (*Synechocystis*) in order to study the little-known cooperative effects of lipids and carotenoids (Cars). Electron microscopic investigations confirmed that in the absence of xanthophylls the S-layer of the cellular envelope is missing. In wild-type (WT) cells, as well as the xanthophyll-less (RO), polyunsaturated lipid-less (AD), and the newly constructed ROAD mutants the lipid and Car compositions were determined by MS and HPLC, respectively. We found that, relative to the WT, the lipid composition of the mutants was remodeled and the Car content changed accordingly. In the mutants the ratio of non-bilayer-forming (NBL) to bilayer-forming (BL) lipids was found considerably lower. Xanthophyll to β-carotene ratio increased in the AD mutant. *In vitro* and *in vivo* methods demonstrated that saturated, monounsaturated lipids and xanthophylls may stabilize the trimerization of Photosystem I (PSI). Fluorescence induction and oxygen-evolving activity measurements revealed increased light sensitivity of RO cells compared to those of the WT. ROAD showed a robust increase in light susceptibility and reduced recovery capability, especially at moderate low (ML) and moderate high (MH) temperatures, indicating a cooperative effect of xanthophylls and polyunsaturated lipids. We suggest that both lipid unsaturation and xanthophylls are required for providing the proper structure and functioning of the membrane environment that protects against light and temperature stress.

© 2017 Elsevier B.V. All rights reserved.

1. Introduction

Lipids, as important constituents of photosynthetic membranes, are key actors in forming dynamic bilayers [34,44]. In cyanobacteria thylakoids are dominant membrane structures, therefore their lipid composition is similar to that of the total cellular membranes [50]. Thylakoids are the sites of oxygenic photosynthesis in cyanobacteria and plants and their lipid composition is unique and highly conserved [7,70]. They include mainly galactolipids, such as monogalactosyldiacylglycerol (MGDG) and digalactosyldiacylglycerol (DGDG), the sulfolipid sulfoquinovosyldiacylglycerol (SQDG), and the phospholipid phosphatidylglycerol (PG). In cyanobacteria the MGDG biosynthetic precursor monoglucosyldiacylglycerol (MGlcDG) is also present [51]. An epimerase can convert glucolipids to galactolipids, and this enzyme has recently been identified in cyanobacteria [3].

The physical behavior of different membrane lipid classes is determined by their head group structure. MGDG and DGDG, together with MGlcDG, have neutral head groups, while SQDG and PG are anionic lipids, bearing one negative charge [70]. Interestingly, MGDG, the

most abundant galactolipid of thylakoids, and MGlcDG are typical non-bilayer-forming (NBL) lipids. They have a cone-like shape, having a small head group and long polyunsaturated tails, which are able to form in aqueous medium an inverted hexagonal structure known as hexagonal II phase [56]. The other lipid classes (DGDG, SQDG and PG) are typical lamellar bilayer-forming (BL) lipids, having a bigger head group and more cylindrical shape [22]. A certain ratio of NBL to BL lipids is crucial for functional membranes [20]. Fine tuning of the MGDG/DGDG ratio makes thylakoid membranes extremely dynamic and flexible to cope with various environmental stress factors [7]. The relatively high NB lipid content in photosynthetic membranes, compared to e.g. plant mitochondrial membranes [48], is needed to accommodate their relatively high protein content. The high protein to lipid ratios of thylakoids [61] can be attributed to extremely large protein complexes of the photosynthetic apparatus, which assist in photosynthetic electron transport.

Behavior of the lipids depends not only on their head groups but also on the saturation level of their fatty acid tails [70]. In cyanobacteria the fatty acyl chain length varies from 14 to 18 carbon atoms (C14–C18), and the number of double bonds also varies from zero to four, leading to saturated, monounsaturated and polyunsaturated fatty acids [43]. In cyanobacteria there is a strong specificity of the fatty acyl group esterification to the sn-positions of the glycerol backbone. Saturated and cis-unsaturated fatty acids with chains of C18 are mainly esterified to the sn-1 position, while the sn-2 position is strongly preferred by C16 esterification [43,52].

Desaturases are enzymes responsible for introducing double bonds at specific sites of the fatty acyl chains, increasing their unsaturation level [35,36]. In cyanobacteria the desaturases DesC, DesA, DesB and DesD catalyze desaturation at the $\Delta 9$, $\Delta 12$, $\omega 3$ and $\Delta 6$ positions, respectively. DesC can exist in two forms, namely DesC1 and DesC2 [5,52]. Genetic tools allow manipulating the unsaturation in membrane glycerolipids of Synechocystis sp. PCC6803 (Synechocystis) in a stepwise manner, by inactivating particular genes that encode the above mentioned desaturases [64].

The level of membrane lipid unsaturation is influenced by changes in the growth temperature, allowing regulation of the fluidity that is necessary for the photosynthetic functions of cyanobacteria [37,45]. When the fluidity of the membrane is modified by decreased temperature, plants and cyanobacteria maintain membrane homeostasis by increasing the number of double bonds in the glycerolipids [45].

X-ray crystallography revealed localization of membrane lipids around and within the main photosynthetic complexes, Photosystem I (PSI) and Photosystem II (PSII) [19,21,68]. These complexes are embedded in the lipid bilayer, therefore specific lipid-protein interactions are very important for maintaining their proper structure and function [10]. Thylakoid lipids have important roles in maintaining the structures of PSII and PSI, as well as in ensuring the proper functioning of the electron transport and chloroplast biogenesis processes [26,41]. Polyunsaturated lipids can protect the photosynthetic machinery from low temperature photoinhibition [15]. It has been suggested that the lipid unsaturation can stabilize photosynthetic complexes exposed to heat stress [14]. Polyunsaturated fatty acids are also important in protecting the photosynthetic machinery against salt stress [1]. Remodeling, reorganization of the lipid content in thylakoid membranes is essential for the survival of cyanobacteria under various stress conditions. It has been demonstrated that Synechocystis cells are capable of retailoring an exogenously added artificial lipid to suit their physiological demands [32].

Carotenoids (Cars), the other key components of photosynthetic membranes, are also hydrophobic, neutral, lipid-like molecules with multiple conjugated double bonds [18]. In cyanobacteria two main forms are present: carotene (β-carotene) and its oxygenated derivatives, xanthophylls [12,30,62,65]. They are parts of the lipid bilayers, and are also associated with proteins in the main photosynthetic complexes. Up to now β-carotene is the only Car that has been found in crystallized forms of the photosynthetic reaction centers [21,68]. Despite their hydrophobic character, Cars can form water soluble fractions when associated with the so-called orange carotenoid proteins [23,54], or the very recently identified helical carotenoid proteins [40].

Cars are multi-functional [74]. They take part in the light-harvesting processes [60] and assembly of the PSII photosynthetic complex [58], modulate membrane structures and protect them from environmental stress factors [11,72]. They are also required for PSII dimerization and PSI trimerization in Synechocystis [65]. Not only Cars but also elevated temperature can stabilize PSI trimers [25]. Whereas in plants PSI exists only in monomeric form [6], in cyanobacteria PSI trimers are also present [17]. In some thermophilic cyanobacteria tetramers could be found [33]. A recent study of tetrameric PSI suggests that these supercomplexes may be stabilized by Cars or lipids [55]. Carotenes may also influence the structure and function of phycobilisomes [65, 69,74]. Cars are also vital for the PSII function [74]. The ΔcrtRO xanthophyll-deficient Synechocystis shows increased sensitivity to high light [53]. A recent study of this mutant highlights the role of zeaxanthin and echinenon in the protection of PSII against high-light-induced photoinhibition, especially during the recovery processes [30]. A very recent paper suggests that moderate heat stress might also enhance the repair of PSII affected by photoinhibition [67].

Glycerolipids, together with Cars, are present at structurally and functionally important sites of the PSI and PSII, and they have determining roles in these pigment-protein complexes [59]. Therefore, investigating lipid-carotenoid-protein interactions in photosynthetic membranes is an intriguing new field of research. During the present study we constructed a multiple mutant of Synechocystis, designated ROAD, which is deficient not only in xanthophylls, but also in polyunsaturated lipids. This strain proved to be a powerful tool for investigating the biochemical background underlying the cooperation between the effects of lipids and Cars. In the mutant cells we could observe remodeling of lipids and reorganization of the Car content. The NBL to BL lipid ratio decreased significantly in the mutant compared to that of the WT. ROAD and WT cells showed distinct compositions and ratios of lipid species. Xanthophyll to β-carotene ratios changed substantially. We suggest that membrane dynamics, biochemical processes like remodeling of lipids and restructuring of Cars, are necessary to stabilize membrane structures in order to ensure optimal functioning of the photosynthetic apparatus, especially under environmental stress conditions. Our results also highlight the possible role of saturated and monoene lipids in stabilizing PSI trimers. Our present study points out the cooperative roles, in some cases additional or synergic effects, of xanthophylls and polyunsaturated lipids in alleviating high light, moderate low (ML) and moderate high (MH) temperature stress effects.

2. Materials and methods

2.1. Organisms and growth conditions

WT and the following mutant strains of Synechocystis sp. PCC6803 were used in this study: RO, AD, ROAD and PsaL. In RO mutant [65] crtR and crtO genes are inactivated, and therefore it is xanthophyll-less. In AD mutant [64] desA and desD genes are interrupted, and therefore it is polyunsaturated lipid-less. In PsaL mutant [25] psaL gene was inactivated, and therefore it is PSI trimer-less.

WT and mutant strains were grown photoautotrophically in BG11 medium [2] supplemented with 5 mM HEPES-NaOH (pH 7.5), at 30 °C under continuous white light illumination at an intensity of $40 \, \mu mol$ photons $m^{-2} \, s^{-1}$. The mutant strains were grown in the presence of following antibiotics: RO ($40 \, \mu g \, ml^{-1}$ kanamycin and spectinomycin), AD ($40 \, \mu g \, ml^{-1}$ kanamycin and $10 \, \mu g \, ml^{-1}$ chloramphenicol), ROAD ($40 \, \mu g \, ml^{-1}$ kanamycin and spectinomycin, $10 \, \mu g \, ml^{-1}$ chloramphenicol and $30 \, \mu g \, ml^{-1}$ erythromycin), and PsaL ($40 \, \mu g \, ml^{-1}$ kanamycin and spectinomycin). Cultures were aerated on a gyratory shaker operating at 100 rpm. The AD and RO mutants were kindly donated

by N. Murata (National Institute for Basic Biology, Okazaki, Aichi, Japan) and K. Masamoto (Kumamoto University, Japan), respectively.

2.2. Mutant generation, transformation of cells

The RO mutant had been created by introducing kanamycin and spectinomycin cassettes into the coding regions of the *crtR* and *crtO* genes, respectively. To generate the ROAD mutant, the coding regions of the *desA* and *desD* genes were amplified by PCR. An erythromycin cassette was introduced to the *Hin*dIII site of *desA*, whereas *desD* was interrupted by a chloramphenicol resistance gene at the *Msc*I site. These resulting DNA constructs were used to transform the RO strain. Complete segregation of the ROAD mutant cells was confirmed by PCR.

2.3. Experimental design

In order to follow temperature stress responses of the WT and mutant strains we transferred the cultures grown at 30 °C to 25 °C or 35 °C. The duration of temperature stress treatments was three days. This was chosen because AD and ROAD cells are extremely light sensitive at 25 °C. For WT cells 30 °C is the optimum growth temperature [64]. The temperatures 25 °C and 35 °C are considered only ML or MH, compared to the optimal temperature.

To study responses to combined temperature and light stress the cells were subjected to 3 h of high light treatment (800 μmol photons $m^{-2} s^{-1}$) at different growth temperatures (25 °C/30 °C/35 °C). For photoinhibition experiments the density of the cultures was set to $OD_{750} = 0.4$. In combined temperature treatment and high light-induced photoinhibition experiments we carried out physiological measurements before the onset of photoinhibition (designated 0), and after 1, 2 and 3 h of high light exposure (designated 1, 2, 3, respectively). After 3 h of photoinhibition we returned the cells to the normal (40 μmol photons $m^{-2} s^{-1}$) light intensity at the respective temperatures and assayed recovery of the cells. Physiological measurements were performed after 1, 3 and 24 h (designated R1, R3, R24, respectively). In experiments with ROAD mutant WT, RO, AD and PsaL cultures served as controls.

2.4. Electron microscopy

For transmission electron microscopy (TEM) the harvested cells were fixed in 1% paraformaldehyde and 1% glutaraldehyde for 4 h at 4 °C and post-fixed in 1% osmium tetroxide. The samples were dehydrated in aqueous solutions of increasing ethanol concentrations, and then embedded in Spurr resin. Following polymerization, 85–90 nm ultrathin sections were cut by a Reichert Ultracut E ultramicrotome (Leica, Wetzlar, Germany). According to the standard procedure, the sections were treated with uranyl acetate and lead citrate and subjected to electron microscopy using a Zeiss EM 902 electron microscope (Carl Zeiss AG, Oberkochen, Germany).

For scanning electron microscopy (SEM) the cells were filtered on poly-L-lysine-coated polycarbonate filters, then fixed in 2.5% glutaraldehyde for 4 h at 4 °C and post-fixed in 1% osmium tetroxide. The samples were dehydrated in aqueous solutions of increasing ethanol concentrations, critical point dried, covered with 10 nm gold by a Quorum Q150T ES sputter and observed in a JEOL JSM-7100F/LV scanning electron microscope. Cell volumes were calculated from the measured diameters of spherical-shaped cells. WT cell volume was taken 100%.

2.5. Lipid analysis

Total lipids were extracted from intact cyanobacterial cells according to Welti et al. [73] with small modifications. Cells ($OD_{750} = 50$) were centrifuged and transferred to 2 ml preheated isopropanol with 0.01% butylated hydroxytoluene and incubated for 20 min at 70 °C, to protect the lipids from phospholipase activity. Afterwards, combined lipid

extraction was performed. After incubation with isopropanol 1 ml chloroform and 0.3 ml of water were added. The tubes were shaken for 1 h at room temperature, followed by the removal of the chloroform phase containing the lipid extract. The extraction step was repeated once with 3 ml of chloroform/methanol (2:1) containing 0.01% butylated hydroxytoluene by 1 h of agitation at room temperature. The remaining cell debris were transferred to a filter paper and heated overnight at 105 °C and weighed. The weights of these dried, extracted cells are the "dry weights" of the cyanobacterial cells. The dry weights ranged from 5 to 14 mg. The combined lipid extracts were washed once with 1.5 ml of chloroform and 0.5 ml of 1 M KCl and then once with 1 ml of water. The solvent was evaporated under nitrogen, and the lipid extract was dissolved in 0.5 ml of chloroform/methanol (2:1) and stored at −80 °C. Before shipping the samples in dry ice the solvent was evaporated and the tube was filled with nitrogen.

Lipidomic analysis of these total lipid extracts was performed at the Kansas Lipidomics Research Center Analytical Laboratory, using their tandem MS-based method (see: https://www.kstate.edu/lipid/analytical_laboratory/lipid_profiling/index.html).

By using known amounts of internal standards the amounts of lipids were quantitated as normalized signals/mg dry weight of the cells. The normalized signal/mg dry weight allows comparison of particular compounds between samples, but may not provide an accurate indication of the relative amounts of compounds within a sample. Double bond indices of different lipid classes were calculated similarly as described in Falcone et al. [13], using the following equation [$\sum$(% of normalized signal intensity/mg dry weight of lipid species × no. of double bonds)] / 100. The percentages of normalized signal intensity/mg dry weight of lipid species are averages of three independent biological replicates.

2.6. Determination of cell density and pigment composition

Cell density in the cultures was determined by measuring OD_{750} in a Shimadzu UV-1601 spectrophotometer. Chlorophyll (Chl) concentration was measured by absorbance at 665 nm, using 90% methanol extracts. A_{665} was multiplied by the extinction coefficient 78.74 [39] to calculate the concentration of Chl *a* (μg Chl *a* ml^{-1}). Pigment compositions of the samples were analyzed by a Shimadzu HPLC system. We used the pigment extraction and separation method described by Vajravel et al. [69]. Car derivatives were identified on the basis of both their absorption spectra and retention times. In order to calculate Car to Chl ratios the concentrations of Car species and Chls were calculated from Beer–Lambert's equation using their specific extinction coefficients at 440 nm [38].

2.7. Separation of thylakoid membranes by clear native-PAGE

Membranes were prepared by breaking the cells with zirconia/silica beads in 25 mM MES/NaOH buffer, pH 6.5 containing 10 mM $CaCl_2$, 10 mM $MgCl_2$, and 20% glycerol [8] using a Mini-Beadbeater (BioSpec, USA). For analysis of the membrane complexes the isolated membranes, corresponding to an amount of 4 μg Chl *a*, were solubilized with 1% (*w/v*) *n*-dodecyl-β-D-maltoside and separated on a 4–14% (*w/v*) polyacrylamide linear gradient gel according to Komenda et al. [28]. The cathode buffer contained 0.05% sodium deoxycholate and 0.02% *n*-dodecyl-β-D-maltoside.

2.8. Fractionation of monomeric and trimeric PSI

Monomers and trimers of PSI pigment–protein complexes were separated as described in Domonkos et al. [9], using a Pharmacia fast protein liquid chromatograph (FPLC) equipped with UV absorption and conductivity detectors. Thylakoid membrane fraction was isolated from intact cells and then solubilized with *n*-dodecyl-β-D-maltoside (DM) to obtain the fraction of pigment-protein complexes. This was filtered and loaded onto a MonoQ HR 5/5 column (Amersham-Pharmacia

Biotech). Samples were eluted with a non-linear gradient of 5 to 200 mM MgSO$_4$, with a flow rate of 0.4 ml min^{-1}, as described by Rogner et al. [47]. Absorbance was measured at 280 nm. Fractions of PSI monomers and trimers were identified as described by Domonkos et al. [9].

2.9. Circular dichroism (CD) measurements

The CD spectra were recorded between 350 and 800 nm at room temperature and at 58 °C by a J815 (Jasco) dichrograph with a Peltier module using a bandpass of 5 nm and a resolution of 1 nm at a 500 nm min^{-1} scanning rate with 1 s integration time. The Chl content of the samples was adjusted to 15 mg ml^{-1} and was measured in a Quartz SUPRASIL cuvette (Hellma) with 1 cm optical path length. CD spectra were normalized to Chl red. For heat dependence correlation we recorded 10 cycles (10 min) of each sample at 58 °C. Data were taken at 515 nm, which is the peak maximum of the PSI trimer/monomer region of the CD spectrum.

2.10. Fast Chl a fluorescence (OJIP transient)

Fluorescence measurements were carried out by a Handy-PEA instrument (Hansatech Instruments Ltd., UK) as described by Laczko-Dobos et al. [31]. Chl contents of the samples were set at 20 μg Chl a ml^{-1}. Samples were dark-adapted for 3 min before the measurements. The first reliable measurable point of the fluorescence transient was at 20 μs. This intensity was taken as the F_0 value for the dark-adapted cells.

2.11. Measurement of photosynthetic oxygen-evolving activity

Photosynthetic oxygen-evolving activity from H$_2$O to CO$_2$ in intact cells was measured at room temperature with a Clark-type oxygen electrode (Chlorolab 2 System, Hansatech Instruments, Kings Lynn, UK), as described by Gombos et al. [16]. Samples were dark-adapted for 3 min before the measurements. Oxygen-evolving activity of the cells was measured in the growth medium without centrifugation. Chl concentration was between 3 and 5 μg ml^{-1}. In all measurements a light from a white LED (color temperature 4100 K) was used at a saturating intensity of 500 μmol photons m^{-2} s^{-1}.

3. Results

3.1. Electron microscopic analysis of cell morphology

The effects of altered lipid and Car composition on cell morphology were studied by TEM. We could not detect considerable morphological differences between cells grown at 25 °C, 30 °C or 35 °C. Fig. 1A shows the morphology of WT and mutant cells grown at 25 °C. AD, RO and ROAD cells did not show apparent morphological alterations compared to those of the WT.

The cells of all strains contained 2 to 8 pairs of thylakoids running parallel to the cytoplasmic membrane. The organization of the thylakoid membranes is also similar although, based on measurements of 50 cells, AD seem to contain fewer thylakoid membrane pairs than the WT. Electron micrographs revealed that in RO and ROAD cells the S-layer (Fig. 1A, black arrow) was not detectable.

SEM was used for comparing the shapes of the WT and mutant cells (Fig. 1B). The surfaces of RO and ROAD cells seemed smoother than those of the WT and AD. The diameter of 50 non-dividing WT, RO, AD and ROAD cells were found 1.26 ± 0.09, 1.30 ± 0.08, 1.37 ± 0.09 and 1.30 ± 0.07 μm, respectively. Accordingly, the volumes were calculated as 100% (WT), 111% (RO), 128% (AD) and 110% (ROAD), indicating slight differences in the cell size.

3.2. Mass spectrometric analyses of membrane lipid composition

We studied the lipid composition of whole cells using a lipidomic approach. The applied tandem mass spectrometric method allowed following the changes in membrane lipid content induced by the absence of xanthophylls and polyunsaturated lipids. In addition to Car and lipid deficiency we also tested the effects of temperature stress.
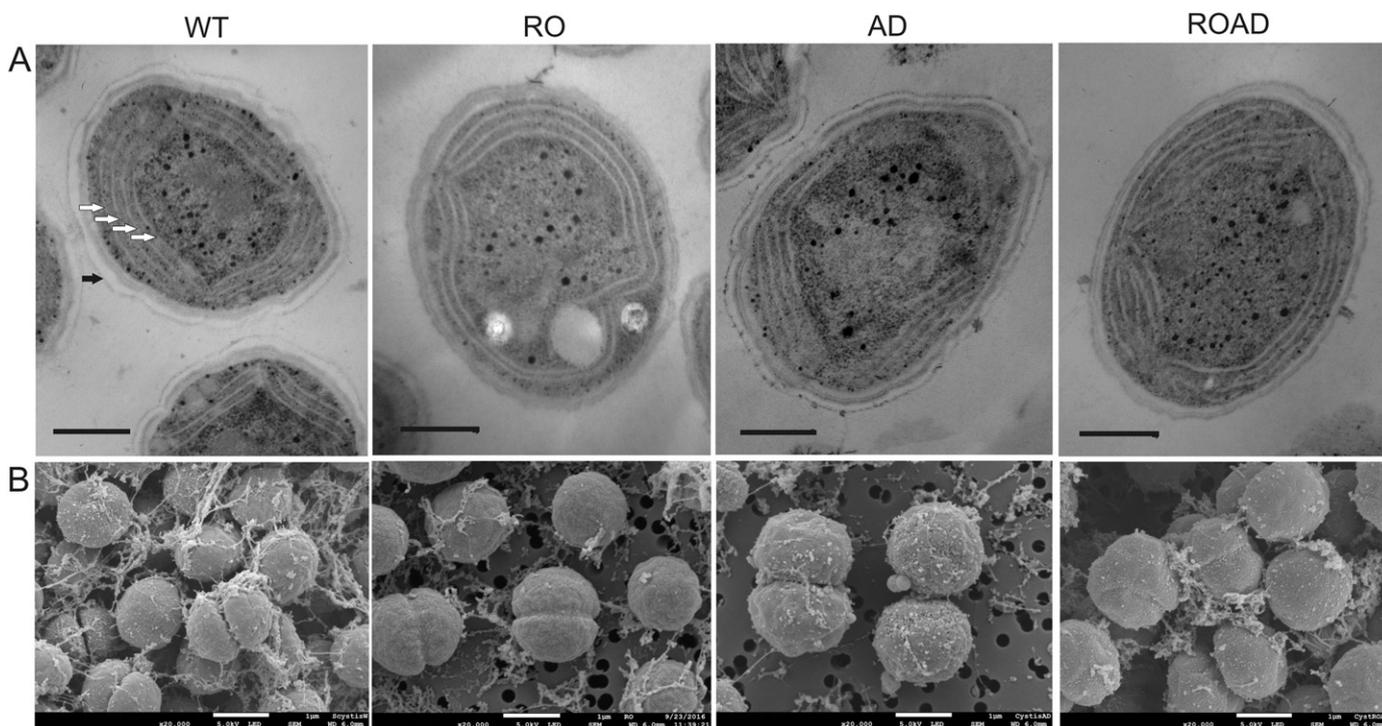
Fig. 1. Electron micrographs of *Synechocystis* wild-type (WT), RO, AD and ROAD cells cultured at 25 °C. (A), TEM micrographs of thin sections. White arrows indicate thylakoid membrane pairs; black arrow shows the S-layer of the cyanobacterial envelope. Bars: 300 nm. (B), SEM images, bars: 1 μm.

3.2.1. Changes in lipid class distribution

In Fig. 2 we compared the distribution of galactolipids (MGDG, DGDG, SQDG) and phospholipids (PG) in WT, as well as RO, AD and ROAD mutant cells grown at different temperatures.

In the WT cells grown at normal temperature the mol percentage distribution of the four main lipid classes were similar to earlier published results [46]. Although in the WT and mutant lines MGDG was the most abundant lipid class, there were noticeable differences in the distribution of this molecule in the Car and lipid mutants, as well as in the cells grown at different temperatures (Fig. 2). Compared to the WT, MGDG levels decreased considerably in the mutants when grown at 30 °C, whereas DGDG level was substantially elevated in RO, and moderately in the AD and ROAD lines (Fig. 2B). Compared to that of the normal growth temperature, the percentage of MGDG decreased further in WT cells grown at 25 °C and 35 °C. In AD and ROAD cells the decrease of MGDG content was more pronounced than in the WT (Fig. 2A and C).

At 30 °C the SQDG levels of the mutants were comparable to that of the WT (Fig. 2B). But when subjected to 25 °C stress, the AD and ROAD lines showed a twofold increase of SQDG content relative to their levels at normal growth temperature (Fig. 2A and C). Interestingly, xanthophyll-deficiency of RO did not alter the SQDG and PG content at normal temperature. However, the absence of polyunsaturated lipids in the AD and ROAD mutants resulted in roughly twofold higher PG levels than that of the WT at the same temperature (Fig. 2B). This increase became
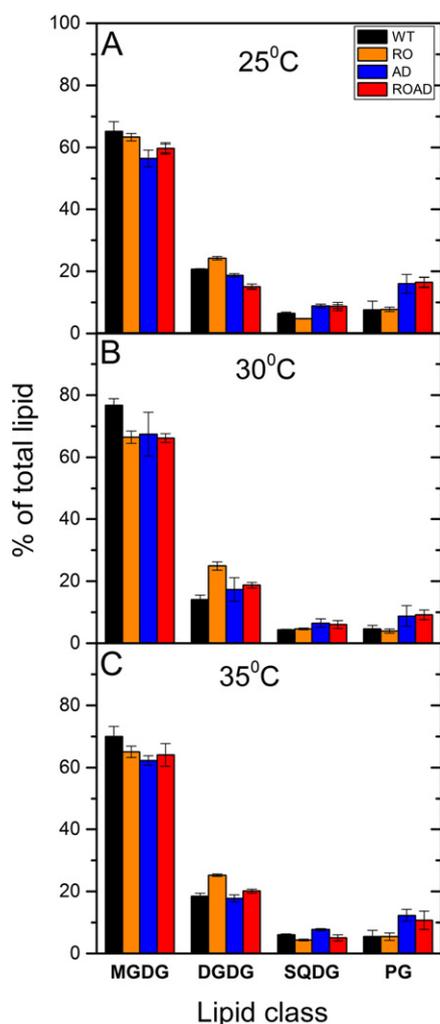
more pronounced when AD and ROAD cells were grown at 25 °C and 35 °C (Fig. 2A and C).

The substantial alterations of lipid class distribution, resulting from the mutations or stress temperatures, are associated with major changes in the NBL to BL lipid ratios. Table 1 shows the NBL to BL lipid ratios of WT and mutant cells, grown at 25 °C, 30 °C and 35 °C.

In the mutants grown at normal temperature we observed a considerable decrease in the NBL/BL ratio, as compared to that of the WT. ML temperature (25 °C) treatment caused a decrease of the NBL/BL ratio even in the WT cells compared to the 30 °C value. At ML temperature only the NBL/BL lipid ratio of the RO strain remained unaffected. However, at ML temperature the decrease of lipid ratios in the AD and ROAD mutants was more pronounced than in the WT. MH temperature (35 °C) had weaker effect than ML temperature on the NBL/BL ratio of the WT. Both the xanthophyll and polyunsaturated lipid mutants showed decreased NBL/BL lipid ratios at 35 °C compared to the WT at the same temperature. It seems that ML and MH temperature has an effect on NBL to BL lipid ratios.

3.2.2. Changes in the composition of lipid species

Tandem mass spectrometry allowed identification and relative quantification of particular lipid species of the above mentioned lipid classes at the level of total acyl chain length and total number of double bonds. Fig. 3 illustrates the main species distribution of MGDG, DGDG, SQDG and PG in the case of the WT and mutant strains grown at 30 °C.

Due to the lack of desaturases (desA and desD), AD and ROAD cells have distinct lipid species pattern compared to those of the WT and the RO mutant. The Car mutation itself also results in changes, mainly in the distribution of the different lipid species, but it does not alter the overall unsaturation level of lipids appreciably. The fatty-acyl composition of lipid species was also determined. The sn-1 and sn-2 positions of the fatty acids were not known; these were estimated on the basis of the already known properties of acyl transferases, which specifically esterify 16-chain fatty acids at the sn-2, whereas 18C-fatty acyls at the sn-1 position [43]. Supplementary Table S1 summarizes fatty acyl compositions of the main lipid species in WT and mutant cells.

Among the lipid classes MGDG and DGDG showed the highest species variety (Fig. 3A and B). In WT cells the most abundant MGDG species were polyunsaturated ones, like 34:3 and 34:4 (Fig. 3A). This is consistent with results obtained in [46]. The RO mutant exhibited similar lipid composition as the WT, but with lower portion of 34:3. The portion of longer fatty-acyl chain containing polyunsaturated MGDG species (36:6, 36:5, 36:4, and 36:3) in RO increased compared to that of those of the WT, as shown in Fig. 3A. AD and ROAD strains lacked polyunsaturated species due to the inactivation of the desaturases. As expected, in these mutants the portion of the monounsaturated MGDG species 34:1 increased dramatically (Fig. 3A). Interestingly, the MGDG 36:2 level was very high in ROAD cells compared to those of the AD, whereas only trace amounts of it were detected in the WT and the RO mutant (Fig. 3A).

DGDG molecular species of the WT and mutant strains are presented in Fig. 3B. These show the same species pattern as seen in the case of MGDG, but with lower levels of polyunsaturated species than in MGDG (DGDG 34:3 decreased and 34:2 increased), while the levels of

Fig. 2. Lipid class distribution in *Synechocystis* wild-type (WT) and RO, AD, and ROAD mutant cells grown at 25 °C (A), 30 °C (B) or 35 °C (C). Error bars show standard deviation in three independent biological replicates.

Table 1
Non-bilayer (NBL) to bilayer-forming (BL) lipid ratios in *Synechocystis* wild-type (WT) and various mutant cells (RO, AD and ROAD) grown at 25 °C, 30 °C and 35 °C.

Temperature	Cyanobacterial strains, NBL/BL lipid ratio ± SD			
	WT(M) ± SD	RO ± SD	AD ± SD	ROAD ± SD
25	1.89 ± 0.26	1.72 ± 0.09	1.30 ± 0.14	1.48 ± 0.11
30	**3.33 ± 0.39**	**1.99 ± 0.18**	**2.17 ± 0.77**	**1.95 ± 0.12**
35	2.35 ± 0.34	1.86 ± 0.15	1.65 ± 0.11	1.80 ± 0.30

SD values are calculated from three independent biological replicates. The main differences are highlighted in bold.
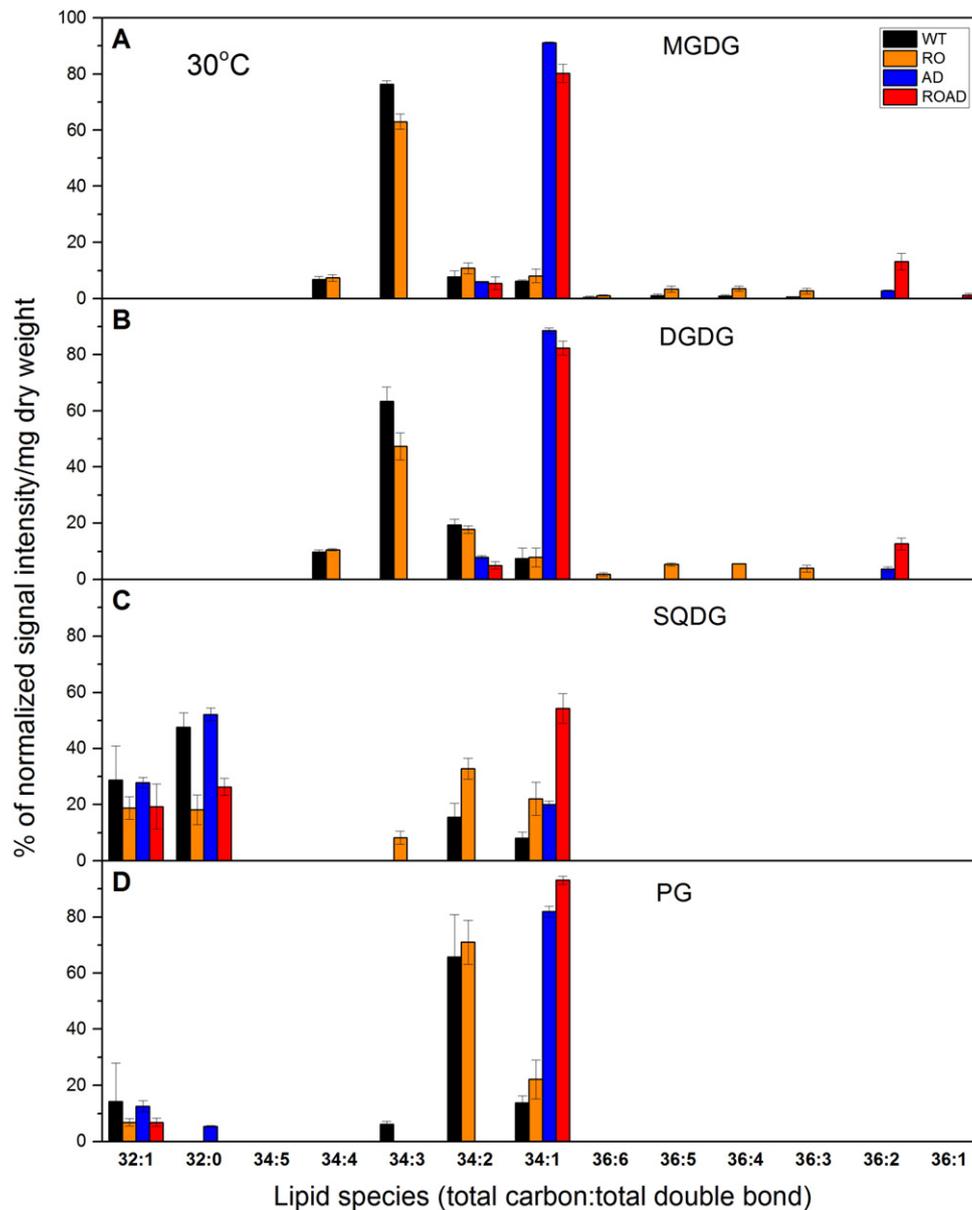
Fig. 3. Fatty acid content of individual lipids in *Synechocystis* wild-type (WT) and mutants (RO, AD, ROAD) grown at 30 °C. (A) MGDG, (B) DGDG, (C) SQDG and (D) PG lipid species. First numbers denote the number of total carbon number, whereas the second numbers those of the total double bond. Data are means $\pm$ SD from three independent biological replicates.

C36 polyunsaturated species noticeably increased in the RO mutant, as compared to the WT.

A comparison of the lipid species patterns of SQDG and PG (Fig. 3C and D) with those of the above mentioned MGDG and DGDG revealed substantial differences. Long carbon chain (C36) species are missing, and the level of polyunsaturation in the C34 species (34:3) is also dramatically decreased. As can be seen in Fig. 3C, new shorter fatty acyl chain-containing SQDG species (32:0 and 32:1) appeared in the WT and all the mutant strains. However, probably due to the absence of xanthophylls, less C32:0 was present in RO and ROAD cells than in the WT and AD. Further abundant species were SQDG 34:1, present in all examined strains, and SQDG 34:2, which was found only in the WT and RO. In RO, AD and ROAD cells the amount of 34:1 increased compared to that of the WT. Among the strains used in this study ROAD contains the highest ratio of SQDG 34:1.

In agreement with earlier results [46], in WT cells 34:2 and 34:1 were the most abundant PG species (Fig. 3D). The RO mutant had similar species distribution as WT cells, dominated by the 34:2 PG species.

By contrast, in the AD and ROAD mutants 34:1 was most dominant PG species.

When grown at ML and MH temperatures, all four strains showed similar lipid species distribution as seen at 30 °C (Supplementary Figs. S1 and S2). Only slight differences could be observed, mainly in the level of SQDG and PG species.

At 25 °C the monounsaturated SQDG (32:1) content dramatically increased in all strains (Supplementary Fig. S1C) compared to their 30 °C levels (Fig. 3C). The higher growth temperature also caused a major increase in the SQDG 32:1 species, mainly in the RO, AD and ROAD mutants (Supplementary Fig. 2C, Fig. 3C). At the ML temperature the SQDG 34:3 and PG 34:3 content dramatically increased in the WT and RO cells, too (Supplementary Fig. 1C and D), while at the MH temperature these lipid species almost disappeared (Supplementary Fig. S2C and D).

Interestingly, the amount of PG 32:1 slightly decreased at the ML and MH temperatures. In the WT and RO 34:2 remained the most dominant PG species, whereas in AD and ROAD PG 34:1 was the most abundant

Table 2
Double bond indices of lipid species belonging to different lipid classes and total lipids of *Synechocystis* wild-type (WT) and mutant strains (RO, AD and ROAD) grown at different temperatures.

Lipid class	Temperature	Cyanobacterial strains, double bond index of lipid species			
		WT	RO	AD	ROAD
MGDG	25	3.09	3.08	1.14	1.14
	30	**2.91**	**2.94**	**1.09**	**1.19**
	35	2.79	2.71	1.09	1.14
DGDG	25	2.99	3.05	1.15	1.15
	30	**2.76**	**2.99**	**1.11**	**1.18**
	35	2.73	2.76	1.11	1.16
SQDG	25	0.97	1.55	0.78	0.78
	30	**0.68**	**1.31**	**0.48**	**0.74**
	35	0.51	1.11	0.48	0.69
PG	25	2.06	2.06	1.00	1.00
	30	**1.78**	**1.71**	**0.95**	**1.00**
	35	1.75	1..72	0.95	1.00
Total lipid	25	9,12	9.75	4.07	4.06
	30	**8.13**	**8.95**	**3.63**	**4.10**
	35	7.78	8.31	3.63	3.99

Double bond indices were calculated as described in the Materials and methods. The main differences are highlighted in bold.

(Supplementary Figs. S1D and S2D), as in the cells of normal growth temperature.

After determining the species distribution of lipid classes in the WT and mutant lines at the different temperatures we were curious whether the removal of xanthophylls and/or temperature stress can influence the overall saturation level in the membranes. If so, we wanted to determine the proportional contributions of the different lipid classes to the total membrane saturation levels. Therefore, we calculated the double bond indices of different lipid classes in the WT and mutant strains grown at 25 °C, 30 °C and 35 °C (see Table 2). Double bond indices were calculated from percentages of normalized signal/mg dry weight

of their molecular species, as given in Fig. 3 and Supplementary Figs S2 and S3. Table 2 shows considerable differences between the double bond indices of the mutants, compared to those of the WT.

As expected, due to the polyunsaturated lipid deficiency the double bond indices of AD and ROAD cells dropped to less than half of the WT values. Compared to the WT, only a slight increase of the total double bond indices could be observed in the RO strain. This seems to arise from the remarkably high double bond index values of the SQDG species in this mutant. AD and ROAD cells do not show appreciable change in their double bond indices when exposed to temperature stress. By contrast, in RO cells a further increase of these values could be seen at the ML temperature, and a small decrease at the MH temperature. We detected nearly twice higher double bond index values of SQDG in the RO cells grown at 25 °C (Table 2).

3.3. Car composition of the WT and mutant strains

HPLC analysis was used to detect changes in the Car composition resulting from xanthophyll- and polyunsaturated lipid-deficiency. Fig. 4A shows the main Cars identified in the WT and mutant strains grown at normal temperature.

In WT cells βcar, Zea, Ech and Myx were the most abundant Cars, confirming earlier results [11,30,65]. AD showed similar Car composition to the WT. RO and ROAD cells were deficient in xanthophylls. In these mutants βcar was the dominant Car. Due to the mutation the main xanthophylls were missing, only Dmyx a precursor of Myx, was present. Fig. 4B shows differences in the proportions of the main Car types. In all mutants the β-carotene content increased relative to the WT. The ROAD mutant contained less Dmyx than RO.

Interestingly, in AD cells the absence of polyunsaturated lipids resulted in a major increase in the Myx and Ech contents. This gave higher xanthophyll per β-carotene ratios in AD, compared to the WT (Table 3). This ratio is further increased under ML temperature stress (25 °C). MH
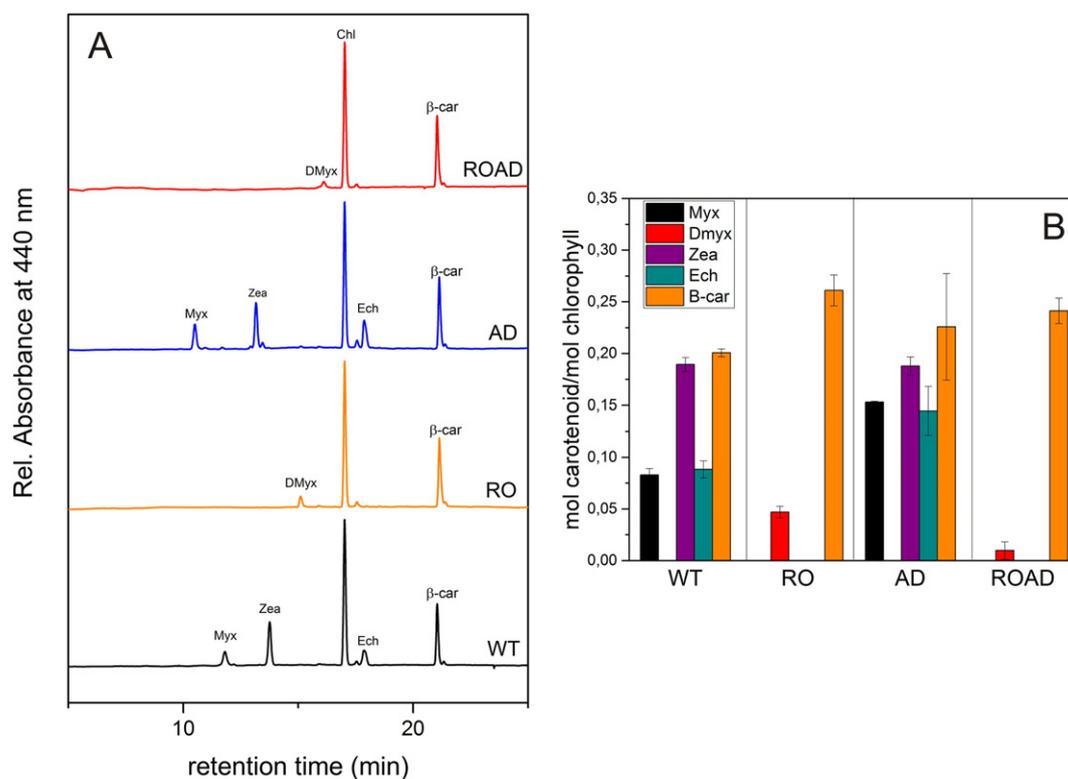
Fig. 4. Carotenoid composition of *Synechocystis* wild-type (WT), RO, AD and ROAD cells analyzed by HPLC. (A) Representative chromatograms showing the identified pigments of the strains. Myx (myxoxanthophyll); Zea (zeaxanthin); Dmyx (deoxymyxoxanthophyll); Chl (chlorophyll); Ech (echinenon); βcar (β-carotene). (B) Relative carotenoid contents (mol carotenoid/mol chlorophyll) of the WT and mutant cells. The values are averages ± SD of three independent biological replicates.

Table 3
Xanthophyll to β-carotene ratios of *Synechocystis* wild-type (WT) and the polyunsaturated lipid-deficient (AD) mutant at 25 °C, 30 °C and 35 °C.

Temperature	Cyanobacterial strain, xanthophyll/β-carotene ± SD	
	WT ± SD	AD ± SD
25	2.24 ± 0.12	2.49 ± 0.06
30	1.8 ± 0.08	2.20 ± 0.36
35	1.91 ± 0.17	2.17 ± 0.13

SD values are calculated from three independent biological replicates.

temperature (35 °C) did not appreciably alter the Car ratios of AD cells compared to the WT.

Supplementary Fig. S3 summarizes the contents of individual Cars of the WT and the AD mutant at optimum, ML and MH temperatures.

Compared to the WT, we observed a considerable increase in the levels of Myx, Zea, Ech, as well as of βcar, in AD cells at 25 °C. In this strain MH temperature caused only a slight increase in the levels of Myx and Ech, relative to the WT (Supplementary Fig. S3).

3.4. Carotenoid and lipid deficiency-induced structural changes in the photosynthetic apparatus

We performed clear native gel electrophoresis to compare how the levels of PSI oligomers are altered in our mutants relative to the WT (Fig. 5). In RO and ROAD cells a decrease of PSI trimers and an increase of PSI monomers was observed, whereas in AD the PSI trimer content was similar to that of the WT. Level of PSII-PSI supercomplexes (RCCS) [4] were not affected in the mutants compared to that of the WT.

To confirm our observation that in the absence of xanthophylls PSI trimers are destabilized, we also analyzed the main photosynthetic complexes using FPLC. Fig. 6 shows the chromatograms obtained from WT and mutant strains pigment-protein complexes.

WT cells had similar PSI trimer to PSI monomer ratio as reported earlier [25], but in the xanthophyll-mutants we observed striking differences in the levels of PSI trimers and monomers, compared to the ratios determined using the clear native gel. RO and ROAD have lower PSI trimer to monomer ratio, whereas AD cells show the same trimer to monomer ratio as the WT, or even somewhat higher than that of the WT. It seems that the stability of PSI trimers also depends on the methods used for isolating the photosynthetic complexes. Therefore,
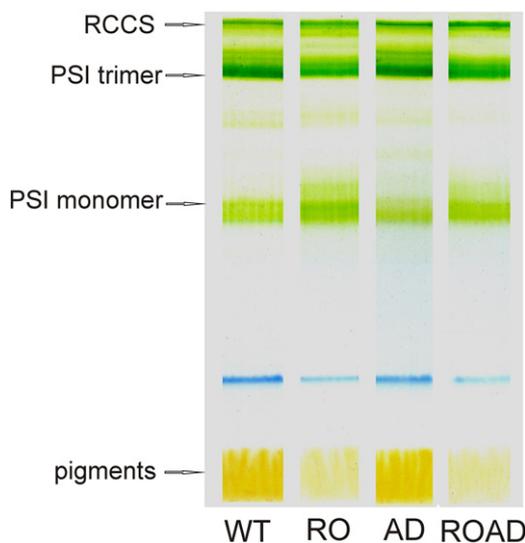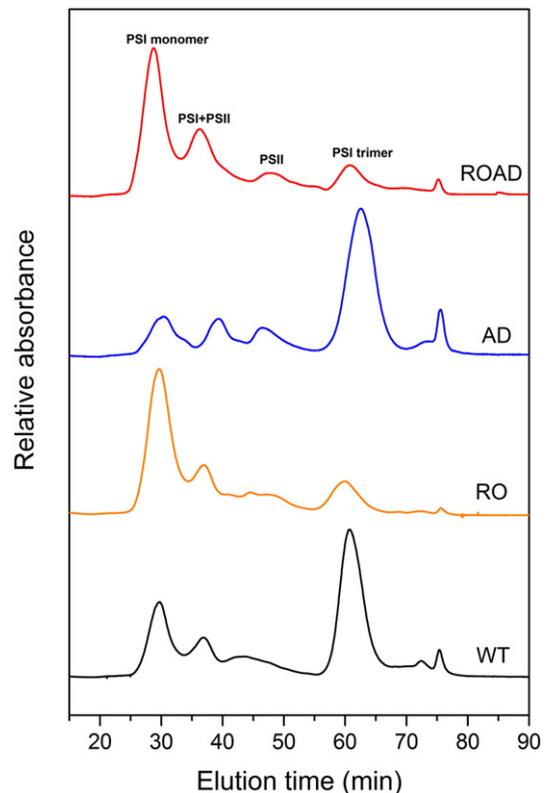
Fig. 6. Oligomers of photosynthetic complexes of *Synechocystis* wild-type (WT), RO, AD and ROAD detected by FPLC. Representative chromatograms showing the main separated fractions: PSI monomers, PSI + PSII (mixture of PSI and PSII complexes), PSII, and PSI trimers.

we further investigated the ratio of PSI trimers and monomers by *in vivo* CD analysis. CD spectra were recorded in whole cells, therefore the PSI trimers were determined in their native environment, without detergent treatment. Fig. 7A shows parallel CD spectra of WT and AD cells, as well as of RO and ROAD cells. To predict the levels of PSI monomers we used PSI trimer-free PsaL-mutant cells as control. We saw that polyunsaturated lipid deficiency alone did not influence the stability of PSI trimers. However, in the absence of xanthophylls (RO and ROAD cells) the 515 nm band decreased considerably, suggesting smaller PSI trimer to monomer ratios than in the WT cells. But, this change was weaker than that seen in the PsaL mutant, as reported earlier [25]. To obtain information on the thermal stability of the PSI complexes we subjected them to heat treatment at 58 °C, as described in Materials and methods. Fig. 7B shows regressive kinetics of the PSI trimers plotted as function of the temperature and time. It shows the instability of PSI trimers in the RO and ROAD strains, as compared to those of the WT and AD.

3.5. Car and lipid deficiency-induced functional changes of the photosynthetic apparatus

3.5.1. Variable Chl a fluorescence (OJIP transients) of the cells

We measured the OJIP transients of WT and mutant cells grown at different temperatures, before and after 3 hour-long photoinhibition, to get information about the efficiency of electron transfer from PSII to PSI. We also followed the recovery processes following 1 h, 3 h and one day of normal light treatment at the same temperatures. OJIP transients of WT, RO, AD and ROAD mutants are presented in Fig. 8. For easier interpretation of the data only 24 hour recovery transients are shown.

In the WT and mutant strains we could distinguish the main phases (OJ, JI, and IP) of the fluorescence curves, as described earlier [31]. At

Fig. 5. Clear native gel of isolated photosynthetic complexes from *Synechocystis* wild-type (WT), RO, AD and ROAD cells grown at 30 °C. The main separated complexes are: RCCS (supercomplex of PSI trimer and PSII core complexes), PSI trimer, and PSI monomer.
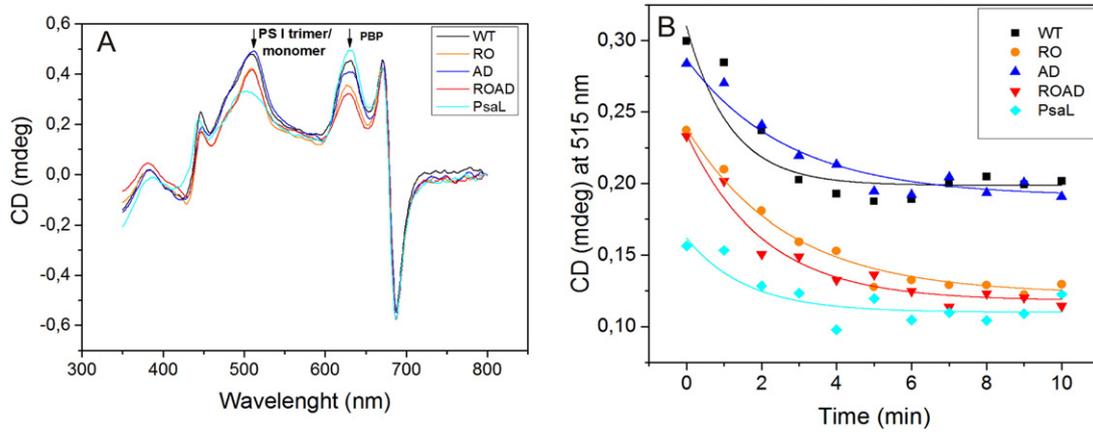
Fig. 7. CD spectra of *Synechocystis* wild-type (WT), RO, AD, ROAD and PsaL cells grown at 30 °C (A), and the effects of 58 °C treatment on the 515 nm band of the WT and mutant cells (B). The main peaks belong to PSI trimer/monomer and PBS (phycobilisomes), respectively.

normal temperature the WT and AD showed similar OJIP transient patterns after high light treatment. At step J a major increase of F_0, and simultaneous increase in fluorescence, could be observed (Fig. 8E and

G). The IP phase became flat, and reached Fm as in the cases when DCMU is added (data not shown). The OJIP curves of RO and ROAD were also similar (Fig. 8F and H), but showed even more pronounced
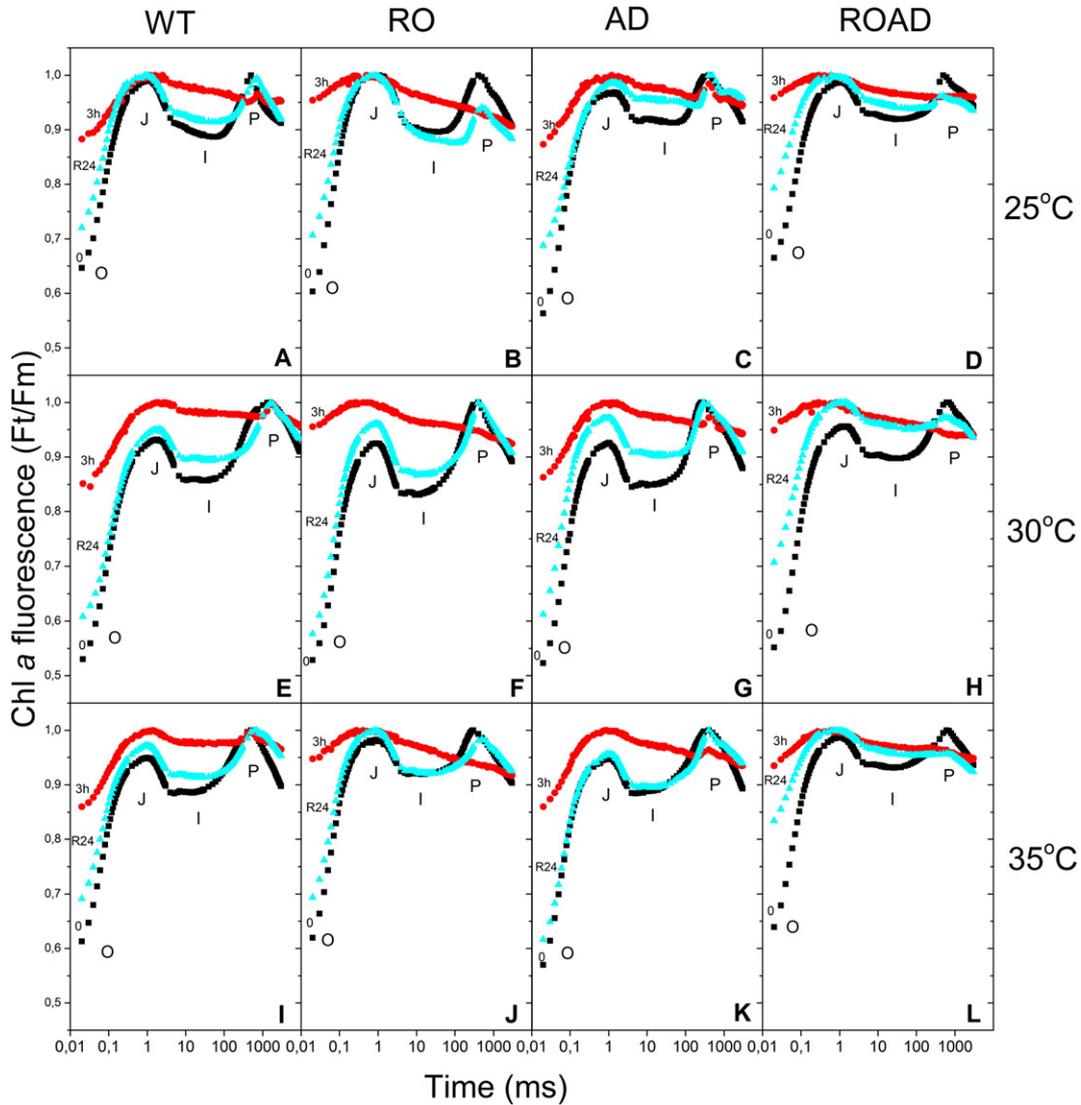
Fig. 8. Effects of temperature and photoinhibitory treatments on Chl *a* fluorescence (OJIP) transients of *Synechocystis* wild-type (WT), RO, AD and ROAD cells. Fluorescence induction curves were normalized to Fm (called Ft/Fm curves). OJIP points correspond to the states before photoinhibition (0, black), after 3 h of high light treatment (3 h, red), and after one day (R24, cyan). Data are plotted along a logarithmic time scale. Cells were grown at 25 °C (A–D), 30 °C (E–H) and 35 °C (I–L), respectively.

F_0 increase and a marked Fm decrease (P phase), relative to WT and AD. Interestingly, while WT, RO and AD recovered almost fully after 24 h, ROAD-cell recovery reached only about 80%. When the cultures were exposed to high light at ML (Fig. 8A–D) and MH (Fig. 8I–L) temperatures we observed similar OJIP transients as seen in the corresponding WT and mutant controls at normal growth temperature (Fig. 8E–H). A striking difference could be observed in the recovery capacity of the WT and the mutants. WT and AD cells showed almost 100% recovery, while RO at 25 °C could not recover properly. ROAD cells showed very low, around 50% recovery rate at both stress temperatures (25 °C and 35 °C).

In Fig. 9 we compare the Fv/Fm values, reflecting the efficiency of PSII, in the WT and the mutants upon combined temperature and high light stress.

At normal growth temperature all strains exhibited similar Fv/Fm values (Fig. 9B). At ML temperature (Fig. 9A) RO and ROAD show appreciable decrease in their Fv/Fm values even before the photoinhibitory treatment. Interestingly, at ML and MH temperatures (Fig. 9A and C) AD had higher Fv/Fm value than the WT. During the 3 h of high light treatment Fv/Fm substantially decreased in all strains, but this effect was most pronounced in RO and ROAD. After 24 h of recovery (R24) the Fv/Fm values of RO and ROAD cells differed from those of the WT and AD, which showed nearly complete recovery. But RO recovery at ML temperature was incomplete (around 80%), and ROAD did not recover completely at any temperature (Fig. 9).

3.5.2. Oxygen-evolving activities of the WT and mutant strains

We measured the photosynthetic oxygen-evolving activity from H_2O to CO_2 of the four *Synechocystis* strains upon temperature stress. Additionally, high light was applied, and the recovery was also followed (Fig. 10).

Following 1 h of high light treatment at 30 °C (Fig. 10A) the oxygen-evolving activity of all strains decreased substantially. After 2 and 3 h of the high light exposure this drop became more pronounced in RO and ROAD. The recovery was faster in the WT, RO and AD, whereas in ROAD it could reach only about 75%. Photoinhibition had a more drastic effect on the oxygen-evolving activity of cells grown at 25 °C and 35 °C (Fig. 10B and C). At 25 °C a 3-hour-long light treatment almost completely abolishes oxygen evolution in ROAD cells. The recovery of ROAD cells was very low at both stress temperatures. These results are consistent with the OJIP transient and F_v/F_m data presented above.

4. Discussion

The protective role of Cars and the importance of lipid unsaturation in photosynthesis are well studied, however cooperative effects of these factors have not been elucidated yet. In the present study we investigated the cooperation between lipids, Cars and proteins in the photosynthetic apparatus. We generated a mutant, *Synechocystis* ROAD, which is xanthophyll- and polyunsaturated lipid-deficient. This strain was used for studying the combined effect of xanthophylls and polyunsaturated lipids on biochemical and physiological processes of photosynthesis in *Synechocystis* cells. In our studies the RO (only xanthophyll-deficient) and AD (only polyunsaturated lipid-deficient) mutants served as references that helped interpreting the mentioned complex cooperative effects.

4.1. The roles of xanthophylls and polyunsaturated lipids in determining cell and membrane structures

Xanthophyll and polyunsaturated lipid deficiency resulted in cell enlargement and slight changes in membrane structures of the cell interior (Fig. 1). Interestingly, the surface layer, or S-layer [57] of the cellular envelope membranes was missing in the xanthophyll-deficient RO and ROAD mutants (Fig. 1A). The S-layer protein of *Synechocystis* was identified as a hemolysin-like protein encoded by the *sll1951* gene [49,66]. It is a 158 kDa glycoprotein that can self-assemble into a lattice structure with hexagonal p6 symmetry around the cell, connecting to the lipopolysaccharides of the outer membrane [57]. The synthesis and assembly of the S-layer protein, as well as its secretion to the cell surface and anchorage in the outer membrane, has not yet been explored. Earlier, Mohamed and co-workers described the absence of S-layer in a ζ-carotene desaturase-inactivated, therefore carotenoid-less, *Synechocystis* mutant [42]. Our observation that RO and ROAD mutants also lack the S-layer supporting the conception that xanthophylls can provide a proper environment in the outer membrane for anchoring S-layer proteins to lipopolysaccharides. These morphological results suggest that both polyunsaturated lipids and xanthophylls might have determinant roles in cell and membrane structures, as well as in ensuring the functions of membrane-imbedded proteins.

Fig. 9. Changes in fluorescence induction parameters (Fv/Fm) of *Synechocystis* wild-type (WT), RO, AD and ROAD during photoinhibitory and recovery treatment at 25 °C (A), 30 °C (B) and 35 °C (C). Fv/Fm values are measured before photoinhibition (0), after 3 h of high light treatment (3), and after 24 h of recovery (R24). Error bars correspond to the means of standard deviation values derived from three independent biological replicates.

Fig. 10. Relative changes in the oxygen-evolving activity during photoinhibitory treatment and recovery of *Synechocystis* wild-type (WT), RO, AD and ROAD cells grown at 30 °C (A), 25 °C (B) and 35 °C (C). 100% activity at 30 °C corresponds to 270 (WT), 277 (RO), 379 (AD) and 193 μmol O_2 mg^{-1} Chl h^1 (ROAD); at 25 °C to 240 (WT), 168 (RO), 190 (AD) and 214 μmol O_2 mg^{-1} Chl h^1 (ROAD); at 35 °C to 265 (WT), 201 (RO), 239 (AD) and 190 μmol O_2 mg^{-1} Chl h^1 (ROAD). Error bars correspond to the means of standard deviation values derived from three independent biological replicates.

4.2. Xanthophyll and polyunsaturated lipid deficiency induces lipid remodeling

Mass spectrometry analyses of total lipid extracts revealed that MGDG is the most abundant lipid in WT *Synechocystis* and in all three studied mutants. This is followed by DGDG as second, and then by two anionic lipids, SQDG and PG. Surprisingly, the relative MGDG content in all mutants decreased by about 10% compared to the WT value. This decrease of MGDG in RO and also in the ROAD mutant was counterbalanced by an increase in the amount of other lipid classes. In the RO mutant this was achieved by increasing the DGDG level, whereas in AD and ROAD not only the DGDG, but also the SQDG and PG contents were substantially enhanced to compensate for the loss of MGDG (Fig. 2). These changes in the lipid class distribution suggest that thylakoid membranes are remodeled differentially in response to the loss of xanthophylls and/or polyunsaturated lipids. In addition to the remodeling observed at optimal growth temperature (Fig. 2B), further fine tuning of lipid classes occurs at ML and MH temperatures (Fig. 2A and C). It seems that these conditions, and especially ML temperature, increased the amount of PG and SQDG, which might have crucial functions in the absence of polyunsaturated lipids.

MGDG is the only NBL lipid of the thylakoids, therefore remodeling resulted in a major change in the NBL to BL lipid ratios (Table 1). In ROAD cells the NBL to BL lipid ratio decreased to about 60% compared

to the WT. Similar NBL to BL lipid ratios was observed when only xanthophylls or polyunsaturated lipids were absent. The AD mutant adapts to the ML temperature by a 20–25% decrease of its NBL lipids, relative to those of the WT, at the same temperature. Simultaneously, the level of BL lipids is noticeably increased to compensate for the loss of NBL species. Such compensatory regulations can ensure proper adjustments of the thylakoid membranes to stress conditions of the environment. In the polyunsaturated and xanthophyll-deficient mutants BL lipids can provide protection and stability of the membrane structure, which are required for the maintenance and stress resistance of photosynthetic functions. The adjustment of NBL to BL ratios is a vital adaptive response of the cells. Our results are in agreement with earlier observations that NBL to BL ratios are crucial determinants of membrane functionality [20].

Remodeling occurred not only at the level of lipid classes, but also by adjusting the proportions and saturation levels of lipid species (Fig. 3). Polyunsaturated long carbon-chain-containing MGDG and DGDG species seem to have specific roles in the absence of xanthophylls. High content of uncommon fatty acid-containing species appear in the absence of both polyunsaturated lipids and xanthophylls. These MGDG and DGDG 36:2 species most probably act as stress lipids.

Surprisingly, the overall saturation level of total lipids are not appreciably changed in the absence of xanthophylls, compared to polyunsaturated lipid-deficient mutants in which overall saturation level is only

65% of the WT (Table 2). A comparison of the saturation levels in the different lipid classes reveals substantial differences in the ways how lipid content was remodeled in the xanthophyll and polyunsaturated lipid mutants. In the WT cells unsaturation level of SQDG and PG dropped by about 80% and 40%, respectively, compared to those of MGDG and DGDG, in agreement with previous reports [43,46]. By contrast, in the RO mutant the unsaturation level of SQDG is about twice higher than that of the WT, and in the AD mutant PG unsaturation remained unchanged. The high unsaturation level of PG and SQDG species seems to be crucial for the survival of the cells under stress conditions by influencing the fluidity of thylakoid membranes.

The effect of low temperatures on the saturation level of glycerolipids is intensely studied in both cyanobacteria and plants. Our results with cells grown at ML and MH temperatures (Supplementary Figs. 1 and 2) confirm that not only extreme, but also small shifts of the growth temperature can induce rearrangements of the lipid content, especially those of PG and SQDG. Remodeling makes the thylakoid membranes extremely flexible and adaptive to stress conditions. Our remodeling results reveal that lipids and Cars can act cooperatively in this process. These results are in good agreement with earlier observations in higher plants [63]. These revealed that the violaxanthin cycle provides protection against high light exposure-induced toxic processes. It has been shown that light-induced membrane rigidification is proportional to the amount of zeaxanthin in the membranes. This phenomenon also highlights the strong correlation between membrane structure and xanthophyll content.

4.3. Changes in membrane Car composition as adaptive response to xanthophyll and polyunsaturated lipid deficiency

Cells compensate for their deficiency in xanthophylls, the main protective agents against reactive oxygen species, by increasing the β-carotene content, consistent with earlier results [30]. In the absence of polyunsaturated lipids not only β-carotene, but also xanthophylls are reorganized in an adaptive response (Fig. 4). Cars, being hydrophobic molecules, are often found in the vicinity of fatty acids. It has been shown that lipids contribute to the Car-binding pockets in cyanobacterial PSII and they might tune the electron transfer processes through these Car-lipid connections [24]. Lipid unsaturation and carotenoid content can influence membrane dynamics and mobility of protein complexes, together with other membranous components [71].

Apparently, in the absence of polyunsaturated lipids the cells become sensitive even at optimal growth temperature, therefore they increase their Myx and Ech content.

When exposed to heat stress, ML temperatures seem to have stronger influence on the reorganization of Car content than MH temperatures (Supplementary Fig. S3). In the AD mutant ML temperature caused not only further increase of Myx and Ech content, but also the accumulation of Zea. Our results provide evidence for the interdependence of lipid and Car contents in the thylakoid membranes.

4.4. Saturated and monounsaturated lipids as well as xanthophylls may stabilize PSI trimers

Xanthophyll deficiency resulted in the partial disintegration of PSI trimers, which could be detected by clear-native electrophoresis and FPLC analyses (Figs. 5 and 6). Similar destabilization of PSI oligomers was observed in the RO mutant by fluorescence methods [65]. For the identification of various protein-pigment complexes FPLC and native electrophoreses are in vitro techniques that require detergent treatments. For studying the aggregation of photosynthetic complexes CD spectroscopy was used as an in vivo method (Fig. 7). The Car-induced CD signal allows distinguishing between the monomeric and trimeric forms of PSI. With this method we observed a trimer to monomer ratio similar to the one obtained with the in vitro methods. Our findings suggest that xanthophylls are needed for providing the optimal

environment for the assembly of photosynthetic reaction centers. Interestingly, in the AD mutant all techniques (FPLC, native electrophoresis and CD) indicated an increase in the PSI trimer content. The AD mutation can increase the sensitivity of the cells to light and ML temperature, thus trimeric PSI may be more advantageous under such stress conditions. It has been shown that among lipids PG has a role in the formation of PSI oligomers [9], and also in connecting CP43 within the PSII core-complex [31]. PG is a crucial lipid in oligomerization and functionality of PSII both in photosynthetic prokaryotes and plants [27,29,41].

The accumulation of trimeric PSI in the absence of polyunsaturated lipids can be explained by the difference between the spatial requirements of saturated, poly- and monounsaturated lipid. The fatty acyl chains of saturated and monounsaturated lipids are straighter and tighter packed than those of the polyunsaturated ones, which have kinks in the tail with bigger spatial requirement. In the case of ROAD we observed a similar enhancement of PSI monomers as in the RO strain. These results suggest additive cooperation between the lipids and carotenoids, in which xanthophylls have a prevailing impact.

4.5. Both polyunsaturated lipids and xanthophylls are required for efficient protection against light and temperature stress

The sensitivity of photosynthesis to high light is enhanced by xanthophyll deficiency, indicating that xanthophylls are major quenchers that protect the photosynthetic machinery from photosynthesis-generated reactive oxygen species.

The lack of polyunsaturated lipids has much less effect on light sensitivity. However, combined xanthophyll and polyunsaturated lipid deficiency has a synergic effect in sensitizing the photosynthetic activities to high light (Figs. 8, 9 and 10). Fluorescence and oxygen-evolving activity measurements suggest that such cooperation between the lipids and xanthophylls are more pronounced at ML and MH temperatures. Both xanthophylls and polyunsaturated lipids affect mainly the recovery processes of membranes and proteins from photoinhibition. Xanthophylls were found to be crucial in the recovery from protein degradation induced by photoinhibitory treatments [30,67]. Polyunsaturated lipids were shown to play important role in recoveries after major drops in the temperature [15]. In contrast to earlier observations, ML and MH temperatures did not have major effects on the recoveries of only xanthophyll, or only polyunsaturated lipid mutants. However, cells with a combined deficiency in lipids and carotenoids were found extremely sensitive to light and suboptimal temperatures. This highlights the cooperation between lipids and Cars in alleviating stress effects.

5. Conclusions

  i. We demonstrated that xanthophyll and polyunsaturated lipid deficiency induces lipid remodeling. As a consequence of lipid remodeling, NBL to BL lipid ratios are substantially modified in the membranes. The removal of xanthophylls induces increase mainly in the DGDG level, while polyunsaturated lipid deficiency results in considerable PG and SQDG accumulation. BL lipids are required for stabilizing the unbalanced and unprotected membranes.

 ii. The removal of polyunsaturated lipids also resulted in the reorganization of the xanthophyll content, increasing the xanthophyll to β-carotene ratio. We demonstrated that lipids and Cars act cooperatively in maintaining and protecting membrane structures.

iii. By using a non-invasive biophysical technique (CD), we demonstrated that deficiencies in both polyunsaturated fatty acids and xanthophylls destabilize PSI trimers. This effect of the xanthophyll deficiency is much more pronounced, as was revealed by a multiple mutant lacking both xanthophylls and polyunsaturated lipids. The exact localization of xanthophylls in the photosynthetic complexes is yet to be determined.

iv. We have shown that the removal of xanthophylls and polyunsaturated lipids increased the sensitivity of PSII to high light-induced

photoinhibition. Cars and lipids were found to have synergic effect in enhancing PSII stability and recovery from photoinhibition, especially at ML and MH temperatures.

In summary, our results revealed that both unsaturated lipids and xanthophylls are required for ensuring the structural and physiological basis of efficient stress protection.

5.1. Future perspective

Better understanding of the influence of lipids and Cars on the functions of photosynthetic membranes will require clarifying the exact molecular mechanisms of their interactions.

Conflict of interest

The author has no conflicts of interest to declare.

Transparency Document

The Transparency document associated with this article can be found, in online version.

Appendix A. Supplementary data

Supplementary data to this article can be found online at http://dx.doi.org/10.1016/j.bbabio.2017.02.002.

References

[1] S.I. Allakhverdiev, Y. Nishiyama, I. Suzuki, Y. Tasaka, N. Murata, Genetic engineering of the unsaturation of fatty acids in membrane lipids alters the tolerance of *Synechocystis* to salt stress, Proc. Natl. Acad. Sci. U. S. A. 96 (10) (1999) 5862–5867, http://dx.doi.org/10.1073/pnas.96.10.5862.

[2] M.M. Allen, Simple conditions for growth of unicellular blue-green algae on plates(1, 2), J. Phycol. 4 (1) (1968) 1–4, http://dx.doi.org/10.1111/j.1529-8817.1968.tb04667.x.

[3] K. Awai, H. Ohta, N. Sato, Oxygenic photosynthesis without galactolipids, Proc. Natl. Acad. Sci. U. S. A. 111 (37) (2014) 13571–13575, http://dx.doi.org/10.1073/pnas.1403708111.

[4] M. Beckova, Z. Gardian, J. Yu, P. Konik, P.J. Nixon, J. Komenda, Association of Psb28 and Psb27 proteins with PSII-PSI supercomplexes upon exposure of *Synechocystis* sp. PCC 6803 to high light, Mol. Plant (2016)http://dx.doi.org/10.1016/j.molp.2016.08.001.

[5] S. Chintalapati, J.S. Prakash, P. Gupta, S. Ohtani, I. Suzuki, T. Sakamoto, N. Murata, S. Shivaji, A novel Delta9 acyl-lipid desaturase, DesC2, from cyanobacteria acts on fatty acids esterified to the sn-2 position of glycerolipids, Biochem. J. 398 (2) (2006) 207–214, http://dx.doi.org/10.1042/BJ20060039.

[6] P.R. Chitnis, Photosystem I, Plant Physiol. 111 (3) (1996) 661–669, http://dx.doi.org/10.1104/pp.111.3.661.

[7] B. Deme, C. Cataye, M.A. Block, E. Marechal, J. Jouhet, Contribution of galactoglycerolipids to the 3-dimensional architecture of thylakoids, FASEB J. 28 (8) (2014) 3373–3383, http://dx.doi.org/10.1096/fj.13-247395.

[8] M. Dobakova, R. Sobotka, M. Tichy, J. Komenda, Psb28 protein is involved in the biogenesis of the Photosystem II inner antenna CP47 (PsbB) in the cyanobacterium *Synechocystis* sp PCC 6803, Plant Physiol. 149 (2) (2009) 1076–1086, http://dx.doi.org/10.1104/pp.108.130039.

[9] I. Domonkos, P. Malec, A. Sallai, L. Kovacs, K. Itoh, G. Shen, B. Ughy, B. Bogos, I. Sakurai, M. Kis, K. Strzalka, H. Wada, S. Itoh, T. Farkas, Z. Gombos, Phosphatidylglycerol is essential for oligomerization of Photosystem I reaction center, Plant Physiol. 134 (4) (2004) 1471–1478, http://dx.doi.org/10.1104/pp.103.037754.

[10] I. Domonkos, H. Laczko-Dobos, Z. Gombos, Lipid-assisted protein-protein interactions that support photosynthetic and other cellular activities, Prog. Lipid Res. 47 (6) (2008) 422–435, http://dx.doi.org/10.1016/j.plipres.2008.05.003.

[11] I. Domonkos, P. Malec, H. Laczko-Dobos, O. Sozer, K. Klodawska, H. Wada, K. Strzalka, Z. Gombos, Phosphatidylglycerol depletion induces an increase in myxoxanthophyll biosynthetic activity in *Synechocystis* PCC6803 cells, Plant Cell Physiol. 50 (2) (2009) 374–382, http://dx.doi.org/10.1093/pcp/pcn204.

[12] I. Domonkos, M. Kis, Z. Gombos, B. Ughy, Carotenoids, versatile components of oxygenic photosynthesis, Prog. Lipid Res. 52 (4) (2013) 539–561, http://dx.doi.org/10.1016/j.plipres.2013.07.001.

[13] D.L. Falcone, J.P. Ogas, C.R. Somerville, Regulation of membrane fatty acid composition by temperature in mutants of *Arabidopsis* with alterations in membrane lipid composition, BMC Plant Biol. 4 (2004) 17, http://dx.doi.org/10.1186/1471-2229-4-17.

[14] Z. Gombos, H. Wada, E. Hideg, N. Murata, The unsaturation of membrane lipids stabilizes photosynthesis against heat stress, Plant Physiol. 104 (2) (1994) 563–567.

[15] Z. Gombos, H. Wada, N. Murata, The recovery of photosynthesis from low-temperature photoinhibition is accelerated by the unsaturation of membrane lipids: a mechanism of chilling tolerance, Proc. Natl. Acad. Sci. U. S. A. 91 (19) (1994) 8787–8791.

[16] Z. Gombos, Z. Varkonyi, M. Hagio, M. Iwaki, L. Kovacs, K. Masamoto, S. Itoh, H. Wada, Phosphatidylglycerol requirement for the function of electron acceptor plastoquinone Q(B) in the Photosystem II reaction center, Biochemistry 41 (11) (2002) 3796–3802.

[17] I. Grotjohann, P. Fromme, Structure of cyanobacterial photosystem I, Photosynth. Res. 85 (1) (2005) 51–72, http://dx.doi.org/10.1007/s11120-005-1440-4.

[18] W.I. Gruszecki, K. Strzalka, Carotenoids as modulators of lipid membrane physical properties, Biochim. Biophys. Acta 1740 (2) (2005) 108–115, http://dx.doi.org/10.1016/j.bbadis.2004.11.015.

[19] A. Guskov, J. Kern, A. Gabdulkhakov, M. Broser, A. Zouni, W. Saenger, Cyanobacterial Photosystem II at 2.9-A resolution and the role of quinones, lipids, channels and chloride, Nat. Struct. Mol. Biol. 16 (3) (2009) 334–342, http://dx.doi.org/10.1038/nsmb.1559.

[20] J.N. Israelachvili, S. Marcelja, R.G. Horn, Physical principles of membrane organization, Q. Rev. Biophys. 13 (2) (1980) 121–200.

[21] P. Jordan, P. Fromme, H.T. Witt, O. Klukas, W. Saenger, N. Krauss, Three-dimensional structure of cyanobacterial Photosystem I at 2.5 A resolution, Nature 411 (6840) (2001) 909–917, http://dx.doi.org/10.1038/35082000.

[22] J. Jouhet, Importance of the hexagonal lipid phase in biological membrane organization, Front. Plant Sci. 4 (2013) 494, http://dx.doi.org/10.3389/fpls.2013.00494.

[23] C.A. Kerfeld, Water-soluble carotenoid proteins of cyanobacteria, Arch. Biochem. Biophys. 430 (1) (2004) 2–9, http://dx.doi.org/10.1016/j.abb.2004.03.018.

[24] J. Kern, A. Guskov, Lipids in Photosystem II: multifunctional cofactors, J. Photochem. Photobiol. B 104 (1–2) (2011) 19–34, http://dx.doi.org/10.1016/j.jphotobiol.2011.02.025.

[25] K. Klodawska, L. Kovacs, Z. Varkonyi, M. Kis, O. Sozer, H. Laczko-Dobos, O. Kobori, I. Domonkos, K. Strzalka, Z. Gombos, P. Malec, Elevated growth temperature can enhance Photosystem I trimer formation and affects xanthophyll biosynthesis in cyanobacterium *Synechocystis* sp PCC6803 cells, Plant Cell Physiol. 56 (3) (2015) 558–571, http://dx.doi.org/10.1093/pcp/pcu199.

[26] K. Kobayashi, Role of membrane glycerolipids in photosynthesis, thylakoid biogenesis and chloroplast development, J. Plant Res. 129 (4) (2016) 565–580, http://dx.doi.org/10.1007/s10265-016-0827-y.

[27] K. Kobayashi, S. Fujii, M. Sato, K. Toyooka, H. Wada, Specific role of phosphatidylglycerol and functional overlaps with other thylakoid lipids in *Arabidopsis* chloroplast biogenesis, Plant Cell Rep. 34 (4) (2015) 631–642, http://dx.doi.org/10.1007/s00299-014-1719-z.

[28] J. Komenda, J. Knoppova, J. Kopecna, R. Sobotka, P. Halada, J.F. Yu, J. Nickelsen, M. Boehm, P.J. Nixon, The Psb27 assembly factor binds to the CP43 complex of Photosystem II in the cyanobacterium *Synechocystis* sp PCC 6803, Plant Physiol. 158 (1) (2012) 476–486, http://dx.doi.org/10.1104/pp.111.184364.

[29] O. Kruse, B. Hankamer, C. Konczak, C. Gerle, E. Morris, A. Radunz, G.H. Schmid, J. Barber, Phosphatidylglycerol is involved in the dimerization of Photosystem II, J. Biol. Chem. 275 (9) (2000) 6509–6514.

[30] Y. Kusama, S. Inoue, H. Jimbo, S. Takaichi, K. Sonoike, Y. Hihara, Y. Nishiyama, Zeaxanthin and echinenone protect the repair of Photosystem II from inhibition by singlet oxygen in *Synechocystis* sp PCC 6803, Plant Cell Physiol. 56 (5) (2015) 906–916, http://dx.doi.org/10.1093/pcp/pcv018.

[31] H. Laczko-Dobos, B. Ughy, S.Z. Toth, J. Komenda, O. Zsiros, I. Domonkos, A. Parducz, B. Bogos, M. Komura, S. Itoh, Z. Gombos, Role of phosphatidylglycerol in the function and assembly of Photosystem II reaction center, studied in a cdsA-inactivated PAL mutant strain of *Synechocystis* sp. PCC6803 that lacks phycobilisomes, Biochim. Biophys. Acta 1777 (9) (2008) 1184–1194, http://dx.doi.org/10.1016/j.bbabio.2008.06.003.

[32] H. Laczko-Dobos, P. Frycak, B. Ughy, I. Domonkos, H. Wada, L. Prokai, Z. Gombos, Re-modeling of phosphatidylglycerol in *Synechocystis* PCC6803, Biochim. Biophys. Acta 1801 (2) (2010) 163–170, http://dx.doi.org/10.1016/j.bbalip.2009.10.009.

[33] M. Li, D.A. Semchonok, E.J. Boekema, B.D. Bruce, Characterization and evolution of tetrameric Photosystem I from the thermophilic cyanobacterium *Chroococcidiopsis* sp TS-821, Plant Cell 26 (3) (2014) 1230–1245, http://dx.doi.org/10.1105/tpc.113.120782.

[34] M. Liberton, H. Pakrasi, Membrane systems in cyanobacteria, in: A. Herrero, E. Flores (Eds.), The Cyanobacteria: Molecular Biology, Genomics and Evolution, Caister Academic Press, Norfolk, UK 2008, pp. 271–285.

[35] D.A. Los, K.S. Mironov, Modes of fatty acid desaturation in cyanobacteria: an update, Life (Basel) 5 (1) (2015) 554–567, http://dx.doi.org/10.3390/life5010554.

[36] D.A. Los, N. Murata, Structure and expression of fatty acid desaturases, Biochim. Biophys. Acta 1394 (1) (1998) 3–15.

[37] D.A. Los, V.V. Zinchenko, Regulatory role of membrane fluidity in gene expression, in: H. Wada, N. Murata (Eds.), Advances in Photosynthesis and Respiration: Lipids in Photosynthesis, Essential and Regulatory Functions, vol 30, Springer, Dordrecht, the Netherlands 2009, pp. 329–348.

[38] R.F.C. Mantoura, C.A. Llewellyn, The rapid-determination of algal chlorophyll and ca-rotenoid-pigments and their breakdown products in natural-waters by reverse-phase high-performance liquid-chromatography, Anal. Chim. Acta 151 (2) (1983) 297–314, http://dx.doi.org/10.1016/S0003-2670(00)80092-6.

[39] J.C. Meeks, R.W. Castenholz, Growth and photosynthesis in an extreme thermophile, *Synechococcus lividus* (Cyanophyta), Arch. Mikrobiol. 78 (1) (1971) 25–41.

[40] M.R. Melnicki, R.L. Leverenz, M. Sutter, R. Lopez-Igual, A. Wilson, E.G. Pawlowski, F. Perreau, D. Kirilovsky, C.A. Kerfeld, Structure, diversity, and evolution of a new fam-ily of soluble carotenoid-binding proteins in cyanobacteria, Mol. Plant 9 (10) (2016) 1379–1394, http://dx.doi.org/10.1016/j.molp.2016.06.009.

[41] N. Mizusawa, H. Wada, The role of lipids in Photosystem II, Biochim. Biophys. Acta 1817 (1) (2012) 194–208, http://dx.doi.org/10.1016/j.bbabio.2011.04.008.

[42] H.E. Mohamed, A.M.L. van de Meene, R.W. Roberson, W.F.J. Vermaas, Myxoxanthophyll is required for normal cell wall structure and thylakoid organiza-tion in the cyanobacterium, *Synechocystis* sp strain PCC 6803, J. Bacteriol. 187 (20) (2005) 6883–6892, http://dx.doi.org/10.1128/Jb.187.20.6883-6892.2005.

[43] N. Murata, H. Wada, Z. Gombos, Modes of fatty-acid desaturation in cyanobacteria, Plant Cell Physiol. 33 (7) (1992) 933–941.

[44] R. Nevo, S.G. Chuartzman, O. Tsabari, Z. Reich, D. Charuvi, E. Shimoni, Architecture of thylakoid membrane networks, in: H. Wada, N. Murata (Eds.), Advances in Photo-synthesis and Respiration: Lipids in Photosynthesis, Essential and Regulatory Func-tions, vol 30, Springer Dordrecht, The Netherlands 2009, pp. 295–328.

[45] I. Nishida, N. Murata, Chilling sensitivity in plants and cyanobacteria: the crucial contribution of membrane lipids, Annu. Rev. Plant Physiol. Plant Mol. Biol. 47 (1996) 541–568, http://dx.doi.org/10.1146/annurev.arplant.47.1.541.

[46] N. Plohnke, T. Seidel, U. Kahmann, M. Rogner, D. Schneider, S. Rexroth, The prote-ome and lipidome of *Synechocystis* sp PCC 6803 cells grown under light-activated heterotrophic conditions, Mol. Cell. Proteomics 14 (3) (2015) 572–584, http://dx.doi.org/10.1074/mcp.M114.042382.

[47] M. Rogner, P.J. Nixon, B.A. Diner, Purification and characterization of Photosystem-I and Photosystem-II core complexes from wild-type and phycocyanin-deficient strains of the cyanobacterium *Synechocystis* Pcc-6803, J. Biol. Chem. 265 (11) (1990) 6189–6196.

[48] R. Sadre, M. Frentzen, Lipids in plant mitochondria, in: H. Wada, N. Murata (Eds.), Advances in Photosynthesis and Respiration: Lipids in Photosynthesis, Essential and Regulatory Functions, vol 30, Springer, Dordrecht, The Netherlands 2009, pp. 57–70.

[49] T. Sakiyama, H. Ueno, H. Homma, O. Numata, T. Kuwabara, Purification and charac-terization of a hemolysin-like protein, Sll1951, a nontoxic member of the RTX pro-tein family from the cyanobacterium *Synechocystis* sp strain PCC 6803, J. Bacteriol. 188 (10) (2006) 3535–3542, http://dx.doi.org/10.1128/Jb.188.10.3535-3542.2006.

[50] I. Sakurai, J.R. Shen, J. Leng, S. Ohashi, M. Kobayashi, H. Wada, Lipids in oxygen-evolving Photosystem II complexes of cyanobacteria and higher plants, J. Biochem. 140 (2) (2006) 201–209, http://dx.doi.org/10.1093/jb/mvj141.

[51] N. Sato, Is monoglucosyldiacylglycerol a precursor to monogalactosyldiacylglycerol in all cyanobacteria? Plant Cell Physiol. 56 (10) (2015) 1890–1899, http://dx.doi.org/10.1093/pcp/pcv116.

[52] N. Sato, H. Wada, Lipid biosynthesis and its regulation in cyanobacteria, in: H. Wada, N. Murata (Eds.), Advances in Photosynthesis and Respiration: Lipids in Photosyn-thesis, Essential and Regulatory Functions, vol 30, Springer, Dordrecht, The Nether-lands 2009, pp. 157–177.

[53] L. Schafer, A. Vioque, G. Sandmann, Functional in situ evaluation of photo synthesis-protecting carotenoids in mutants of the cyanobacterium *Synechocystis* PCC6803, J. Photochem. Photobiol. B 78 (3) (2005) 195–201, http://dx.doi.org/10.1016/j.jphotobiol.2004.11.007.

[54] A. Sedoud, R. Lopez-Igual, A.U. Rehman, A. Wilson, F. Perreau, C. Boulay, I. Vass, A. Krieger-Liszkay, D. Kirilovsky, The cyanobacterial photoactive orange carotenoid

[55] protein is an excellent singlet oxygen quencher, Plant Cell 26 (4) (2014) 1781–1791, http://dx.doi.org/10.1105/tpc.114.123802.

[55] D.A. Semchonok, M. Li, B.D. Bruce, G.T. Oostergetel, E.J. Boekema, Cryo-EM structure of a tetrameric cyanobacterial Photosystem I complex reveals novel subunit interac-tions, Biochim. Biophys. Acta 1857 (9) (2016) 1619–1626, http://dx.doi.org/10.1016/j.bbabio.2016.06.012.

[56] G.G. Shipley, J.P. Green, B.W. Nichols, The phase behavior of monogalactosyl, digalactosyl, and sulphoquinovosyl diglycerides, Biochim. Biophys. Acta 311 (4) (1973) 531–544.

[57] J. Smarda, D. Smajs, J. Komrska, V. Krzyzanek, S-layers on cell walls of cyanobacteria, Micron 33 (3) (2002) 257–277 (doi:Pii S0968-4328(01)00031-2).

[58] O. Sozer, J. Komenda, B. Ughy, I. Domonkos, H. Laczko-Dobos, P. Malec, Z. Gombos, M. Kis, Involvement of carotenoids in the synthesis and assembly of protein sub-units of photosynthetic reaction centers of *Synechocystis* sp PCC 6803, Plant Cell Physiol. 51 (5) (2010) 823–835, http://dx.doi.org/10.1093/pcp/pcq031.

[59] O. Sozer, M. Kis, Z. Gombos, B. Ughy, Proteins, glycerolipids and carotenoids in the functional Photosystem II architecture, Front. Biosci. (Landmark Ed) 16 (2011) 619–643, http://dx.doi.org/10.2741/3710.

[60] K. Stamatakis, M. Tsimilli-Michael, G.C. Papageorgiou, On the question of the light-harvesting role of beta-carotene in Photosystem II and Photosystem I core com-plexes, Plant Physiol. Biochem. 81 (2014) 121–127, http://dx.doi.org/10.1016/j.plaphy.2014.01.014.

[61] B. Szalontai, Y. Nishiyama, Z. Gombos, N. Murata, Membrane dynamics as seen by Fourier transform infrared spectroscopy in a cyanobacterium, *Synechocystis* PCC 6803 — the effects of lipid unsaturation and the protein-to-lipid ratio, BBA-Biomembranes 1509 (1–2) (2000) 409–419, http://dx.doi.org/10.1016/S0005-2736(00)00323-0.

[62] S. Takaichi, M. Mochimaru, Carotenoids and carotenogenesis in cyanobacteria: unique ketocarotenoids and carotenoid glycosides, Cell. Mol. Life Sci. 64 (19–20) (2007) 2607–2619, http://dx.doi.org/10.1007/s00018-007-7190-z.

[63] F. Tardy, M. Havaux, Thylakoid membrane fluidity and thermostability during the operation of the xanthophyll cycle in higher-plant chloroplasts, Biochim. Biophys. Acta 1330 (2) (1997) 179–193.

[64] Y. Tasaka, Z. Gombos, Y. Nishiyama, P. Mohanty, T. Ohba, K. Ohki, N. Murata, Targeted mutagenesis of acyl-lipid desaturases in *Synechocystis*: evidence for the important roles of polyunsaturated membrane lipids in growth, respiration and photosynthesis, EMBO J. 15 (23) (1996) 6416–6425.

[65] T.N. Toth, V. Chukhutsina, I. Domonkos, J. Knoppova, J. Komenda, M. Kis, Z. Lenart, G. Garab, L. Kovacs, Z. Gombos, H. van Amerongen, Carotenoids are essential for the as-sembly of cyanobacterial photosynthetic complexes, BBA-Bioenergetics 1847 (10) (2015) 1153–1165, http://dx.doi.org/10.1016/j.bbabio.2015.05.020.

[66] C. Trautner, W.F.J. Vermaas, The sll1951 gene encodes the surface layer protein of *Synechocystis* sp strain PCC 6803, J. Bacteriol. 195 (23) (2013) 5370–5380, http://dx.doi.org/10.1128/Jb.00615-13.

[67] M. Ueno, P. Sae-Tang, Y. Kusama, Y. Hihara, M. Matsuda, T. Hasunuma, Y. Nishiyama, Moderate heat stress stimulates repair of Photosystem II during photoinhibition in *Synechocystis* sp. PCC 6803, Plant Cell Physiol. 57 (11) (2016) 2417–2426, http://dx.doi.org/10.1093/pcp/pcw153.

[68] Y. Umena, K. Kawakami, J.R. Shen, N. Kamiya, Crystal structure of oxygen-evolving Photosystem II at a resolution of 1.9 Angstrom, Nature 473 (7345) (2011) 55–U65, http://dx.doi.org/10.1038/nature09913.

[69] S. Vajravel, L. Kovacs, M. Kis, A.U. Rehman, I. Vass, Z. Gombos, T.N. Toth, Beta-caro-tene influences the phycobilisome antenna of cyanobacterium *Synechocystis* sp. PCC 6803, Photosynth. Res. (2016)http://dx.doi.org/10.1007/s11120-016-0273-7.

[70] F.J. van Eerden, D.H. de Jong, A.H. de Vries, T.A. Wassenaar, S.J. Marrink, Character-ization of thylakoid lipid membranes from cyanobacteria and higher plants by mo-lecular dynamics simulations, BBA-Biomembranes 1848 (6) (2015) 1319–1330, http://dx.doi.org/10.1016/j.bbamem.2015.02.025.

[71] F.J. van Eerden, T. van den Berg, P.W. Frederix, D.H. de Jong, X. Periole, S.J. Marrink, Molecular dynamics of Photosystem II embedded in the thylakoid membrane, J. Phys. Chem. B (2016)http://dx.doi.org/10.1021/acs.jpcb.6b06865.

[72] Z. Varkonyi, K. Masamoto, M. Debreczeny, O. Zsiros, B. Ughy, Z. Gombos, I. Domonkos, T. Farkas, H. Wada, B. Szalontai, Low-temperature-induced accumula-tion of xanthophylls and its structural consequences in the photosynthetic mem-branes of the cyanobacterium *Cylindrospermopsis raciborskii*: an FTIR spectroscopic study, Proc. Natl. Acad. Sci. U. S. A. 99 (4) (2002) 2410–2415, http://dx.doi.org/10.1073/pnas.042698799.

[73] R. Welti, W.Q. Li, M.Y. Li, Y.M. Sang, H. Biesiada, H.E. Zhou, C.B. Rajashekar, T.D. Williams, X.M. Wang, Profiling membrane lipids in plant stress responses — role of phospholipase D alpha in freezing-induced lipid changes in *Arabidopsis*, J. Biol. Chem. 277 (35) (2002) 31994–32002, http://dx.doi.org/10.1074/jbc.M205375200.

[74] T. Zakar, H. Laczko-Dobos, T.N. Toth, Z. Gombos, Carotenoids assist in cyanobacterial Photosystem II assembly and function, Front. Plant Sci. 7 (2016) 295, http://dx.doi.org/10.3389/fpls.2016.00295.